

NN31157.32

MARS

Monitoring
Agroecological
Resources with
Remote Sensing &
Simulation

MAPPING AGROECOLOGICAL
ZONES AND TIME LAG IN
VEGETATION GROWTH BY
MEANS OF FOURIER
ANALYSIS OF TIME SERIES
OF NDVI IMAGES

REPORT 32

Agricultural Research Department
The Winand Staring Centre for Integrated Land,
Soil and Water Research

sc-dlo



Wageningen (The Netherlands), 1991

32/447(32) 20 e*

BIBLIOTHEEK
STARINGGEBOUW

**Mapping agroecological zones and time lag in vegetation growth by
means of Fourier analysis of time series of NDVI images**

**M. Menenti,
S. Azzali,
W. Verhoef,
R. van Swol**

Report 32

DLO The Winand Staring Centre, Wageningen, The Netherlands, 1991

4 DEC. 1991

usn sub 117*

ABSTRACT

Menenti, M., S. Azzali, W. Verhoef, R. van Swol. *Mapping agroecological zones and timelag in vegetation by means of Fourier analysis of time scenes of NDVI images*. Wageningen (The Netherlands), DLO The Winand Staring Centre, Report 32. 46 pp.; 14 Figs; 1 Table.

The objective of this research is to present a method which gives a quantitative meaning to general concepts such as "variability of vegetation growth", "growth cycle" and "early or late growing season". This is accomplished by applying Fourier analysis to time series of 10-day composites of Normalized Difference Vegetation Index (NDVI) images of Zambia and Somalia. Time series of NDVI images are de-convoluted in a set of harmonic functions having different periods (or frequency). The amplitude of each harmonic gives the contribution of NDVI variation in time to the actual observations; for each harmonic the timelag with respect to the origin of time in the observations is obtained.

Since the technique is applied on a pixel by pixel basis, maps are obtained of amplitude and time-lag for each period. Different techniques are compared to map zones wherein vegetation development is similar and which will be termed "isogrowth" zones. The obtained results indicate that differences in vegetation development among map units of an existing agro-climatic map are not significant, while reliable differences are observed among the map units obtained by means of the here described procedure.

Keywords: Normalized Difference Vegetation Index (NDVI), Fourier analysis, Zambia, Somalia, remote sensing, agroecological zones

ISSN 0924-3062

This report will also be published as BCRS report no. 9122.

© 1991 DLO The Winand Staring Centre for Integrated Land, Soil and Water Research,
Postbus 125, 6700 AC Wageningen (The Netherlands)
Phone: +31837074200; fax: +31837024812; telex: 75230 VISI-NL

DLO The Winand Staring Centre is continuing the research of: Institute for Land and Water Management Research (ICW), Institute for Pesticide Research, Environment Division (IOB), Dorschkamp Research Institute for Forestry and Landscape Planning, Division of Landscape Planning (LB), and Soil Survey Institute (STIBOKA).

No part of this publication may be reproduced or published in any form or by any means, or stored in a data base or retrieval system, without the written permission of DLO The Winand Staring Centre.

Project 4110

[485mr/09.91]

CONTENTS

	Page
PREFACE	7
SUMMARY	9
1 INTRODUCTION	11
2 THEORY	15
3 QUALITATIVE RESULTS: MAPPING ZONES HAVING SIMILAR VEGETATION GROWTH DYNAMICS	19
4 QUANTITATIVE RESULTS: FOURIER SPECTRA OF ZONES HAVING SIMILAR VEGETATION GROWTH DYNAMICS	31
5 MAPPING AGROECOLOGICAL ZONES	35
6 EVALUATION OF AUTOMATIC CLASSIFICATION METHODS	39
7 CONCLUSIONS	41
REFERENCES	43
FIGURES	
1 NDVI temporal pattern of one pixel, Eastern Province, Zambia; data points are dekadic measurements from 1 September 1983 till 31 August 1984	17
2a Agroclimatic Map of Zambia	19
2b Agroecological map of Somalia	20
3 Colour composite of amplitude images at P=36 respectively P=18 (red), Zambia Sept. 1983-August 1984	23
4 Colour coded image of phase values of the yearly component of growth cycle, Zambia Sept. 1983-August 1984	25
5 Colour composite of amplitude and phase of the yearly (P=36 dek.) component of the growth cycle; growing season 1983-1984	27
6 Colour composite of amplitude images at P=36 dek. P=18 dek. and P=9 dek.; Somalia, Jan. 1984 to Dec. 1984	29
7 Fourier spectrum of NDVI time serie; Zambia, 1 Sept. 1983-31 Aug. 1984; dominant components at P=36, 18 and 9 dek. are considered only; a scale factor of 4 respectively of 9 has been applied to values at P=18 respectively 9	31
8 Fourier spectrum of NDVI time serie; Zambia, 1 Sept. 1983-31 Aug. 1984; dominant components at P=36, 18 and 9 dek. are considered only; a scale factor of 4 respectively of 9 has been applied to values at P=18 respectively 9	32

	Page
9 Mean phase values of agroclimatic zones of dominant components of vegetation growth at periods P=36, 18 and 9 dekades; Zambia growing season 1 Sept. 1983 to 31 Aug. 1984	32
10 Fourier spectrum of NDVI time serie; Somalia, 1 Jan. 1984-31 Dec. 1984; dominant components at P=36, 18 and 9 dek. are considered only; a scale factor of 4 respectively of 9 has been applied to values at P=18 respectively 9	33
11 Map of iso-growth zones obtained by applying a maximum likelihood classification algorithm; attributes: amplitude and phase of yearly component (P=36 dek.) of growth cycle, Zambia Sept. 1983-August 1984	36
12 Map of iso-growth zones obtained by applying a maximum likelihood classification algorithm; attributes: amplitude of yearly P=36 dek.) and six-monthly component (P=18 dek.) of growth cycle, Zambia Sept. 1983-August 1984	37
13 Fourier spectrum (amplitude) of NDVI time serie; Zambia, 1 Sept. 1983-31 Aug. 1984; dominant components at P=36, 18 and 9 dek. are considered only; a scale factor of 4 respectively of 9 has been applied to values at P=18 respectively 9	39
14 As Fig. 13; isogrowth zones are the ones of the map presented in Fig. 12	40
 TABLE	
Case-studies of low resolution satellite data used to detect crop condition	12

PREFACE

In 1989 and 1990 a Fast Fourier Transform algorithm applicable to the analysis of time series of satellite images has been developed and tested. The idea to develop this method arose for a complete different problem from the one which is dealt with in this Report. Originally the objective was to account for variations in local solar time between elements of image lines covering several thousands kilometers, such as in the METEOSAT Thermal InfraRed ones. After the first experiences done with METEOSAT-TIR images it was decided to apply the same method to time series of Normalized Difference Vegetation Index (NDVI) images. The results of this first study are presented in this Report.

SUMMARY

In this Report examples of applications of a Fast Fourier Transform algorithm are presented to the analysis of time series of images of Normalized Difference Vegetation Index (NDVI) values. The examples are based on NDVI observations of Zambia and Somalia during two growing seasons.

For this purpose a method has been developed to give a quantitative meaning to general concepts such as "variability of vegetation growth", "growth cycle" and "early or late growing season".

The theoretical background is derived from well known mathematical and physical aspects of wave-like phenomena. The developed method consists in several steps. A time serie of NDVI images is first transformed into a set of images of amplitude and phase values of waveforms having different periodicity (or frequency). Colour composites of amplitude and phase images in different combinations have been applied to obtain a preliminar, qualitative map of zones wherein development of vegetation is similar in time, which are called "isogrowth" zones in this Report.

A more precise description of the development of vegetation within such "isogrowth" zones has been obtained by taking the mean amplitude and phase values of the periodic components (waveforms) of vegetation development within individual map units. A string of such values at different frequencies gives a very clear characterization of differences in vegetation development among zones. Maximum likelihood image classification has been applied by taking amplitude and phase values as attributes in different combinations.

The significance of the differences in vegetation development among classification results has been assessed by taking mean and standard deviation values of each attribute within each map units. The results presented in this Report prove that maps of agroecological zones based on indicators which are only indirectly related to vegetation growth are rather inaccurate. The latter means that these maps do not provide a reliable distribution of zones wherein development in time of green vegetation is similar. A much better definition of such zones has been obtained on the basis of the Fourier transform of NDVI time series. A clear advantage of the method proposed here is that growth-indicators calculated on the basis of the Fourier transform have a very clear mathematical and physical meaning, which makes further analysis easier.

1 INTRODUCTION

Description of problem

Subdivision of a region into smaller units, where in vegetation develops in a similar way, is required for two different reasons:

- synthetic description of main geographical features of the region;
- estimation of parameters of models applied to describe quantitatively processes as diverse as interaction of land surface with atmosphere or agricultural production.

Such homogeneous units may be mapped indirectly, i.e. on the basis of land properties which affect vegetation development, whereby each particular combination of vegetation growth factors is taken to induce spatially similar development of vegetation in time. Another possibility is to apply air- or spaceborne imagery to map homogeneous vegetation units. A vast array of methods can be applied to this purpose varying from qualitative image interpretation to advanced statistical techniques (Johnson et al., 1987; Iverson and Hendricksen, 1989; Brown and Prevost, 1985; Hendricksen, 1986; Azzali, 1990a). Experience shows that the latter approach does seldom give accurate and objective results. Image classification by either photo interpretation or numeric classification does seldom lead to unique results. The former indirect approach is severely limited by data availability over large areas and by understanding of the ecology of extensive and complex vegetation communities.

Approach

The objective of this research is to present a method which gives a quantitative meaning to general concepts such as "variability of vegetation growth", "growth cycle" and "early or late growing season". This is accomplished by applying Fourier analysis to time series of 10-day composites of Normalized Difference Vegetation Index (NDVI) images. Fourier analysis of time series of meteorological and hydrological observations (Rosini et al., 1974) is a powerful tool to establish the dominant dynamic features of watershed hydrology and climatology.

Time series of NDVI images are de-convoluted in a set of harmonic functions having different periods (or frequency). The amplitude of each harmonic gives the contribution of NDVI variation in time to the actual observations; for each harmonic the time-lag with respect to the origin of time in the observations is obtained. Each harmonic is a component of the "growth cycle" having a precisely defined period; the amplitude values of different harmonics for a given area are an objective measure of "variability of vegetation growth". Finally time-lag values are an exact measure of "earliness or lateness of vegetation growth".

Since the technique is applied on a pixel by pixel basis, maps are obtained of amplitude and time-lag for each period. In this report different techniques are compared to map zones wherein vegetation development is similar and which will be termed "isogrowth" zones.

Table Case-studies of low resolution satellite data used to detect crop condition

Country	Type of agro climatological model	Satellite data	Duration	Remarks	Source
China	-	NOAA-NDVI	1982-1983	NDVI calculated for 9 major agricultural regions	Justice et al., 1985
China	-	NOAA-NDVI-GAC LANDSAT-MSS aerial photographs	1986	assess biomass changes	Morain, 1986
Botswana	-	NOAA-AVHRR GAC-pixel (NDVI)	1983-1984	LANDSAT-MSS images were acquired for ground sampling identification. Regression from NDVI calculated both with MSS and AVHRR data was applied	Prince, 1986
Sahel-Sudan Ethiopia	FAO, 1979	NOAA-AVHRR- NDVI-GAC and LAC data, SMMR data base	1980-1988	Evaluation of drought monitoring and early warning capability by using 1983-85 drought as testcase	Anonymous, 1987
Sahelian countries		LANDSAT-MSS, NOAA-AVHRR, SPOT	1980-1984	JOLIBA Project; radiometric measures on groundtruth plots; phenology and yield data of cultivated crops comparison of satellite data with radiometric measurements	Berg et al., 1984
USA	Meteo crop models	NOAA-AVHRR NDVI	1981-1985	Satellite calibration measurements for biomass production	Boatwright et al., 1986
Sahelian + Horn of Africa countries	AISC/CIAM models	NOAA-AVHRR NDVI	1985-1986	NDVI values utilized for crop yield forecasting. System ready for application	Johnson et al., 1987b
New Zealand	PET with Penman formula, water balance	NOAA-AVHRR	1981-1984	Crop: pasture. Biomass over a very large homogeneous area 1000 sqkm. Collection of daily rainfall data. Not yet routinely applied	Taylor et al., 1985
Canada	Meteo crop yield models	NOAA-AVHRR	1982	Canadian wheat board needs estimates of domestic and foreign wheat production, even if promising results have been given, method is not yet operational	Glick, et al., 1984
Tanzania	-	NOAA-AVHRR in framework of LACIE project	not specified	Constraints: small size fields, intercropping, this applies to AVHRR-GAC	King, 1984
Egypt	-	NOAA-AVHRR NDVI-calculation	1981	Suitable method for the global growing season response but unsuitable for inventory of a specific crop yield or specific crop acreage	Tucker et al., 1984

The particular meteorological conditions of Zambia (Huygen, 1989), where the onset of the rainy season moves across the country from NE to SW create favourable conditions for a first test of the method presented here. Rainfall-induced development of vegetation follows a similar spatial and temporal pattern which can be quantitatively described in terms of Fourier components.

State of art

During the past ten years much effort has been spent on developing methods to apply low resolution satellite data to assess vegetation conditions within extensive regions mostly in Africa. Many case-studies have been presented in literature and the Table gives a summary of some of those; 90% of literature here proposed deals with the monitoring of vegetation development by means of NOAA-AVHRR-NDVI images in Africa, the rest shows some applications in Europe and North-America.

NOAA-AVHRR data allow the monitoring of very extensive areas at reasonable cost showing the temporal variability of vegetation resources by using vegetation indices (Justice et al., 1985, 1986a,b; Tucker et al., 1984, 1985a; Prince, 1986; Townshend et al., 1985, 1986; Henricksen, 1986; Hielkema et al., 1986; Johnson et al., 1987).

Methods using NOAA-AVHRR-NDVI time series have also been developed to assess the vegetative biomass and indirectly crop yield (Lagouarde et al., 1985; Seguin, 1985; Tucker et al., 1985b; Justice et al., 1986b; Hiernaux et al., 1986; Hansen and Soegaard, 1987; Philipson and Teng, 1988; Kennedy, 1989).

The integration and testing of NOAA-AVHRR-NDVI time series with agrometeorological models has also been attempted to detect more quantitatively crop yield (Taylor et al., 1985; Glick et al. 1984; Boatwright and Whitehead, 1986; Azzali, 1990 b; Henricksen and Durkin, 1986a,b; LeComte et al., 1988) and yield forecasting (Azzali, 1990a; Berkhout et al., 1988).

2 THEORY

The reader is referred to Brandt and Dahmen (1989), Box and Jenkins (1970) and Fourier (1818); here only essential definitions are given.

A time serie of NDVI-images will be indicated as $I(x,y,t)$ where x is pixel number or longitude, y is line number or latitude and t is time measured in dekades (10 days) in this Report. $I(x,y,t)$ can be expressed as a linear combination of elementary periodic functions:

$$I(x,y,t) = \sum_{n=0}^N A_n(x,y) \exp i[w_n t - g_n(x,y)] \quad (1)$$

where w_n is frequency, A_n is amplitude and g_n is phase-lag.

The dependence on (x,y) of phase g_n indicates that the components of the "green wave" (progressively up-greening of vegetation) $I(x,y,t)$ can be thought of as waveforms moving with time across the observed area in exactly the same way as waves in water do.

Each wave, at frequency n , describes the part of vegetation green up which occurs at that frequency.

It is, herefore, useful to introduce the concept of wave-function:

$$f(s,t) = \exp i(w_n t - qs) \quad (2)$$

where s is a generic space coordinate, and q is the wave-vector which is related to the translation velocity v of the wave (phase velocity) through the relation:

$$v = w/q \quad (3)$$

Accordingly, eq. 1 can be re-written in terms of wave-functions:

$$I(x,y,t) = \sum_{n=0}^N A_n(x,y) \exp i[w_n t - q_n(x,y)s] \quad (4)$$

The temporal Fast Fourier Transform algorithm was developed at NLR as a tool for the analysis of time series of images. For a series of coregistered images equally spaced in time, the FFT is computed for each individual pixel and the final result is a series of images containing the amplitudes and phases for the different frequencies. In this way the dynamic behaviour of objects in the image can be studied with greater ease and classification on the basis of differences in dynamic behaviour is facilitated.

A sequence of N real input images results in N complex Fourier coefficient images, but since each coefficient at frequency n , $A(n)$, equals the complex conjugate of $A(N-n)$, the frequencies greater than $N/2$ are redundant for N even and those greater than $(N-1)/2$ for N odd. Also, $A(0)$ is always real for real input and when N is even $A(N/2)$ is real.

In the latter case, the result consists of $N/2+1$ amplitude images and $N/2-1$ phase images, since $A(0)$ and $A(N/2)$ have zero phase.

The number of input images N can take on values like 48 for Meteosat images during the daily cycle, or 36 for NOAA-NDVI 10-day composite images in a yearly cycle. Therefore, an FFT-algorithm for N equal to a power of two cannot be used. Instead, a so-called mixed radix FFT algorithm was chosen (Singleton, 1969) as appropriate for the task. In this case the only restriction is that N should be made up of factors of 2, 3, 4 and 5. The FFT algorithm is faster than the normal Fourier transform because the latter requires a number of operations proportional to N^2 , whereas the former reduces this to approx. N times the number of factors making up N . For $N=48$ these numbers are $48^2 = 2304$ and (when 48 is factored as $4 \times 3 \times 4$) $48 \times 3 = 144$, respectively. This reduction in computation time is achieved by breaking up the calculation in a number of elementary steps, in which FFTs of dimension 2, 3, 4 or 5 are carried out, and by making intelligent use of intermediate results. A further reduction is possible for N even and real input. In that case the N -point FFT on real data is carried out as an $N/2$ -point complex FFT on N complex numbers composed of even samples in the real parts and odd samples in the imaginary parts, followed by some additional processing.

Since in many cases the input data consist of separate image files for the times of observation, it is first necessary to perform a packing operation in order to facilitate the access to the complete series of observations for each individual pixel. This packing operation results in a single file, in which the data are stored in an interleaved format, i.e. each spatial segment (usually a scanline or part thereof) is stored as a group of N records, in which each record represents a time of observation. The temporal FFT-algorithm reads a group of N records into memory, does the FFT on the time dimension of the array for each pixel, and writes the output array to disk as N records, now containing the amplitudes and phases for each frequency.

A final unpacking operation is performed in order to obtain the transformed results as separate image files. The output images are of type byte (0-255) in order to facilitate display. The amplitudes are scaled in order to reduce truncation errors. Scaling is based on the amplitude spectrum of a positive cosine wave, i.e. the idealized course of solar irradiance during the day. In this case the scaling factor for frequency n equals (n^2-1) for the even frequencies, but this was also applied for the odd frequencies. For $n=1$ the scaling factor chosen was 5, which seemed reasonable from inspection of test results. The phases are encoded as integers from zero to 240. Although less appropriate in the case of the NOAA-NDVI imagery, the same scaling was applied with satisfactory results. This algorithm transforms a time serie of NDVI images into a set of amplitude and phase of harmonics having increasing frequency; amplitude and phase images are obtained since the Fourier Transform is applied on a pixel by pixel basis.

To explain in an easier way the above-mentioned theoretical concepts, an example is given. Fig. 1 shows the NDVI pattern of one pixel ($x=139$, $y=88$, Eastern province, Zambia). In particular, individual data points in Fig. 1 are NDVI dekadic measurements during the period 1 September 1983 till 31 August 1984, while the line in Fig. 1 represents the temporal pattern of NDVI calculated using eq. 1 where the amplitude A_n and phase g_n values at three frequencies, w_n ($2\pi/36$, $2\pi/18$ and $2\pi/9$) are obtained for the same pixel.

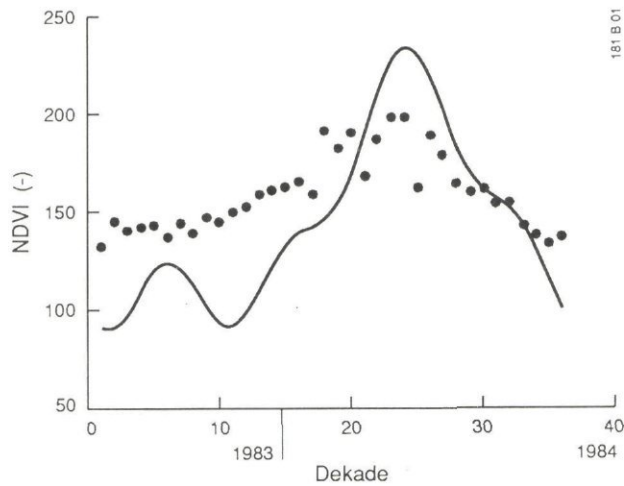


Fig. 1 NDVI temporal pattern of one pixel, Eastern Province, Zambia; data points are dekadic measurements from 1 September 1983 till 31 August 1984, line represents the temporal pattern of NDVI calculated using Eq. 1

The method described above has been applied to the following data sets:

Zambia: 1 September 1983 through 31 August 1984 and

1 September 1984 through 31 August 1985

Somalia: 1 January 1984 through 31 December 1984

1 January 1985 through 31 December 1985

Data is 10 day composites produced at NASA GSFC and re-sampled to a 7.3 x 7.3 km resolution by means of the ARTEMIS system at FAO.

3 QUALITATIVE RESULTS: MAPPING ZONES HAVING SIMILAR VEGETATION GROWTH DYNAMICS

In this Report the term "vegetation dynamics" is meant to indicate a particular combination of amplitude and phase values at different frequencies. In general terms relatively high amplitude values at higher frequencies, i.e. at periods shorter than one year, indicate that secondary growth cycles occur beside the primary, yearly, one. Low phase values at any frequency indicate that the highest NDVI value resulting from that particular growth cycle is observed early in the growing season.

Similarities in vegetation development can be easily detected by combining amplitude and phase images in a colour composite, whereby different colour shades indicate zones wherein vegetation development in time is different.

Results obtained with our method will be compared with:

- Agroclimatic map of Zambia (Schultz, 1974);
- Agroecological map of Somalia (Watson, 1979, 1982, 1985);

These maps are presented in Fig. 2a respectively 2b; results presented in this Section relate to the years 1983-1984 (Zambia) and 1984 (Somalia).

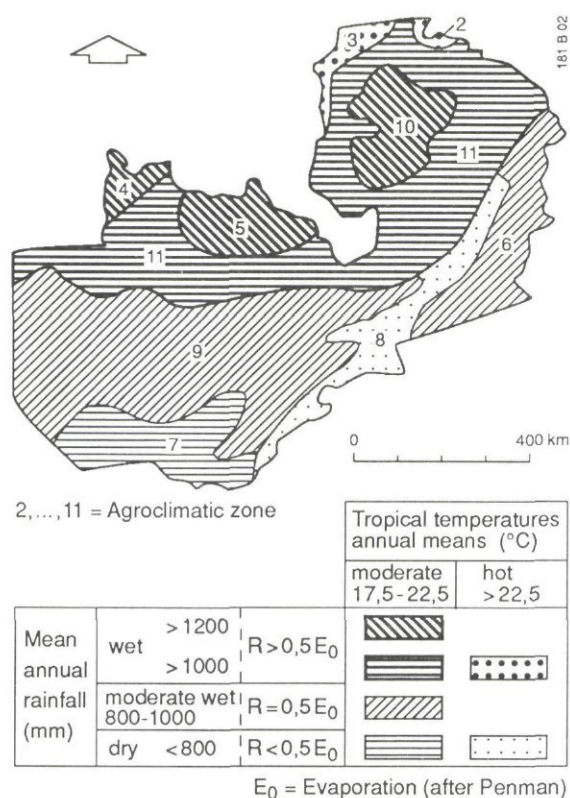


Fig. 2a Agroclimatic map of Zambia (after Schultz, 1974)

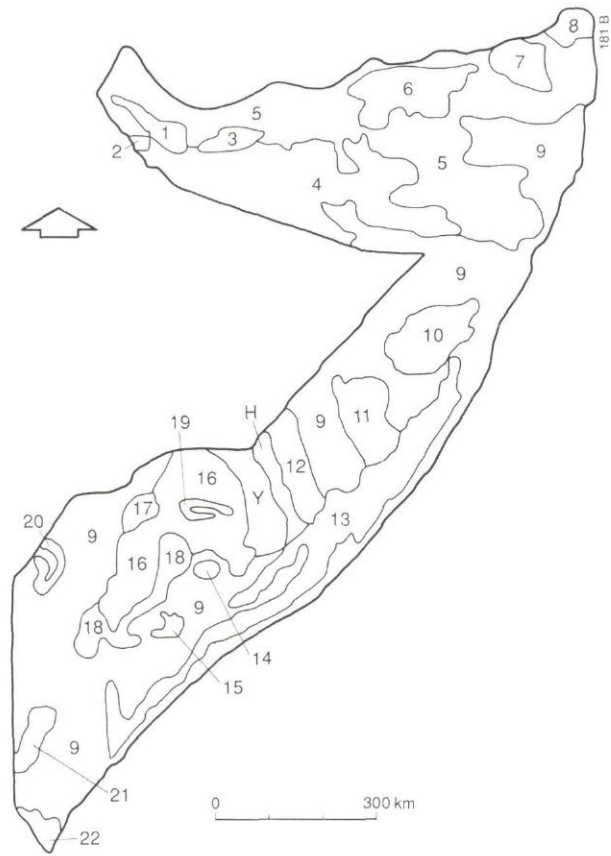


Fig. 2b Agroecological map of Somalia (after Watson, 1979, 1982, 1985)

Legend

Main agroecological zones in Somalia

Class description according to Watson, 1979, 1982, 1985

Class number	Description
1	mixed basement mountain and sandy basement plateau; medium potential for grazers; rainfed cropping possible
2	loamy clay plains; high potential for the grazers; extensive rainfed cropping may be applied
3	volcanic lava (flows and cones); low potential for browsers and grazers
4	sandy plains; medium potential for browsers and grazers
5	limestone and anhydrite, silty limestone plains; low-medium potential for grazers
6	limestone plateau with anhydrite; in limestone plateau high-very high potential for grazers; rainfed crops
7	limestone mountains; medium-low potential for grazers
8	limestone plateau and mountains; low potential for browsers, grazers only seasonally
9	limestone plateau, in the south alluvial plains; low potential for browsers and grazers only seasonally
10	sands over limestone, medium shrubland, limestone ridge pattern
11	sands over limestone, short shrubland, herbland uniform
12	limestone; shrubland, low shrub; low density of rainfed crops
H	herbland
13	stabilized dunes; high density of rainfed crops are present
Y	high crop productivity
14	medium-high potential for browsers and seasonally (WS) for grazers; medium-high forestry potential; rainfed cropping in almost all year and in deep soils
15	as n. 14; rainfed cropping in most year
16	medium-high potential for browsers and seasonally (WS) for grazers; medium-high potential for forestry
17	medium potential for browsers and seasonally for grazers; medium forestry potential; rainfed cropping extensive in deep soil not every year
18	extensive rainfed cropping in almost all year and both in the rain seasons, very high potential for browsers and grazers
19	medium potential for browsers; medium forest potential; rainfed cropping in deep soils
20	sandstone-limestone broken hills and dissected plateau; medium low potential for browsers and seasonally grazers; low forestry potential; rainfed cropping not every year
21	alluvial plains; very high potential for the browsers and seasonally (WS) for grazers with disease control; rainfed cropping in some years; high potential for forestry
22	tidal swamp, sand dunes; very (extremely) high seasonal (DS) potential for browsers and grazers after disease control; rainfed cropping, in almost all years on deep soils and or after drainage; very high potential for forestry

A preliminary analysis of the results obtained for Zambia did show that beside the primary, yearly, vegetation growth cycle a secondary growth cycle having a period of 6 months (18 dekades) is observed. Accordingly, our "isogrowth" zones can be mapped by combining the amplitude images at period $P=36$ and 18 dekades in a colour composite; the result is presented in Fig. 3.

Zones where the amplitude of the yearly cycle is much larger than the one of the six-month cycle are reddish, while zones where the six-month cycle is dominant are greenish. Although some isogrowth zones partly match the zones of the agroclimatic map, the two maps are rather different. At times no difference in vegetation development is observed between different zones in the agroclimatic map. For practical purposes is useful to assess whether vegetation growth is occurring "earlier" or "later" respect to the expected trend at a particular place; a measure of this is provided by phase values. In Fig. 4 an image of the phase $g(x,y)$ at a period of 36 dekades is presented; the meaning of phase is explained by eq. 1: high phase values imply that the maximum value of a particular component of growth cycle is achieved later in the growing season.

Most (i.e. 90%) phase values in Fig. 4 are in the range 12 to 18 dekades; this means that the highest value of the yearly cycle was attained between the beginning of December 1983 (aqua) and end of April 1984 (crimson). Earliness of the primary growth cycle might be considered a more important feature of vegetation growth than the amplitude of the six-month component; iso-growth zones can also be mapped by combining amplitude and phase values of the same component of observed growth, e.g. at $P=36$ dek.

An example is presented in Fig. 5; zones wherein high NDVI values are attained early in the growing season are greenish, while zones, where yearly maximum NDVI values are rather low and are attained late in the growing season, are reddish. The resulting iso-growth zones are rather similar to the ones depicted in Fig. 3; a more detailed comparison of methods to identify iso-growth zones will be presented later in this Report.

Conceptually similar results were obtained for the Somalia case-study, although in this case components at $P=36$, 18 and 9 dek. were considered, because of the different rainfall regime in that country. Rainfall amount and distribution throughout the year differ substantially in the Northern and Southern part of Somalia and up to three rainfall seasons may occur in the South. This is underscored by the large number of iso-growth zones depicted in Fig. 6; in a small fraction of the area (white) vegetation growth is the result of growth cycles at periods $P=36$, 18 and 9 dek. Areas shown in either red, green or blue indicate that only one of these basic cycles prevails.

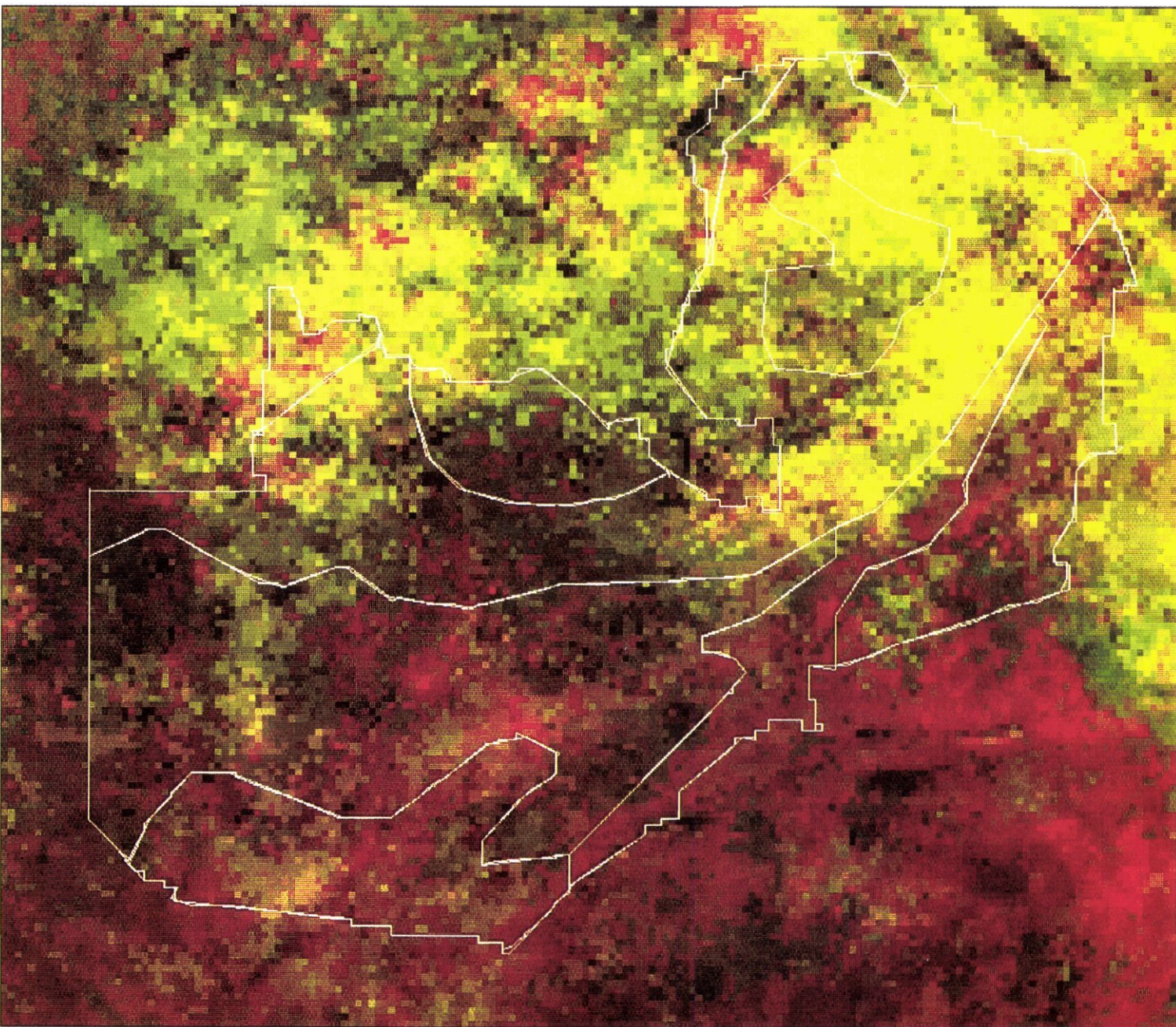


Fig. 3 Colour composite of amplitude images at P=36 (green) respectively P=18 (red), Zambia, Sept. 1983-August 1984; the agroclimatic map of Fig. 2a has been digitized and superimposed as reference

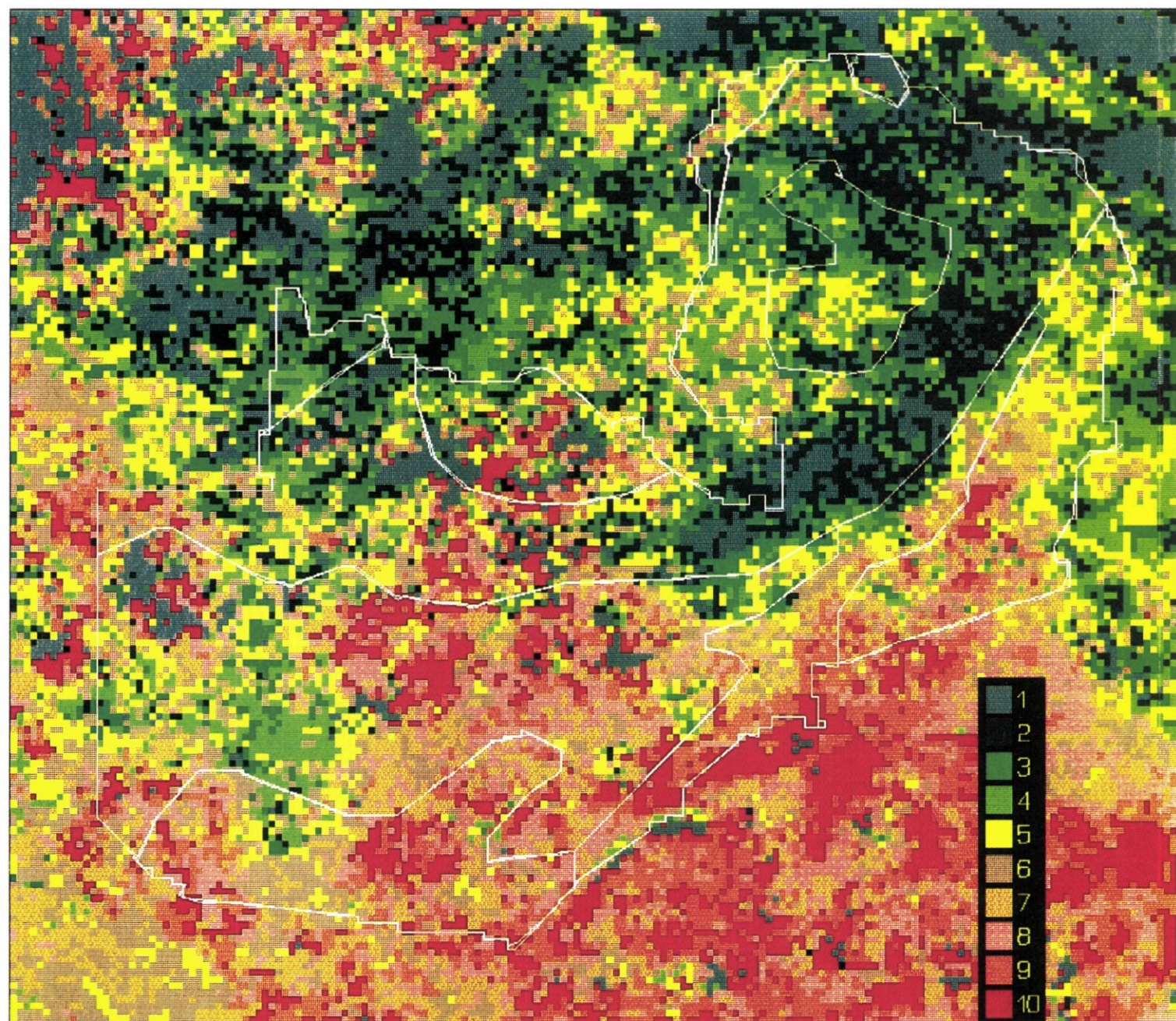


Fig. 4 Colour coded image of phase values of the yearly component of growth cycle, Zambia, Sept. 1983-August 1984; values within a 10-percentile range have been assigned a colour from aqua ($g=0$ through 120 deg.) to crimson ($g>180$ deg.); agroclimatic map (see Fig. 2a) is shown as reference

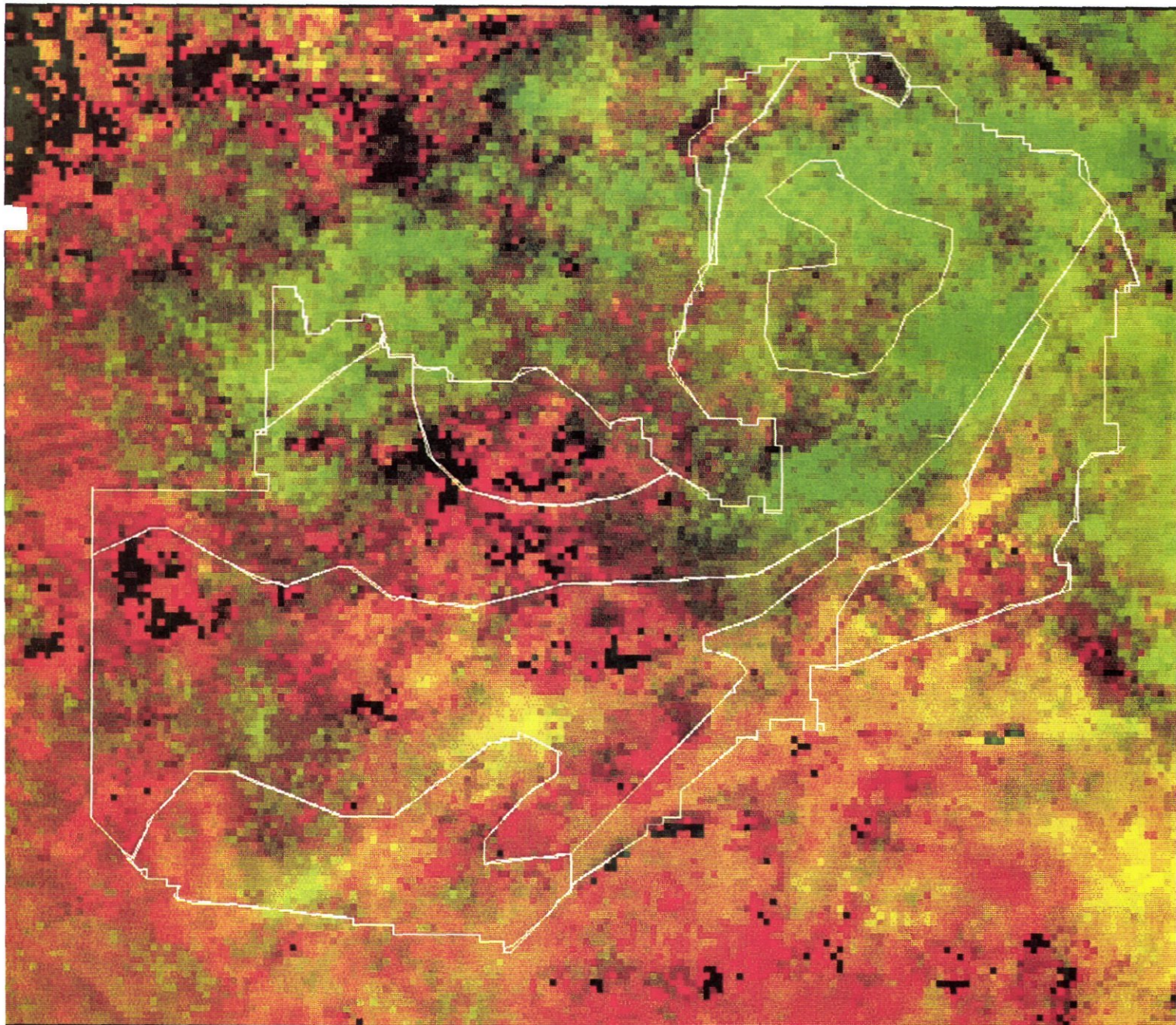


Fig. 5 Colour composite of amplitude (green) and phase (red) of the yearly (P=36 dek.) component of the growth cycle; growing season 1983-1984; agroclimatic map shown as reference



Fig. 6 Colour composite of amplitude images at $P=36$ dek. (red), $P=18$ dek. (green) and $P=9$ dek. (blue); Somalia, Jan. 1984 to Dec. 1984; agroclimatic map (see Fig. 2b) shown as reference

4 QUANTITATIVE RESULTS: FOURIER SPECTRA OF ZONES HAVING SIMILAR VEGETATION GROWTH DYNAMICS

In the previous section images obtained by applying the Fourier transform to the original NDVI time serie have been applied in a qualitative manner to characterize the development of vegetation in time. Here quantitative examples of the practical use of the Fourier transform will be presented.

To this end mean values of amplitude and phase have been calculated for map units of the Agroclimatic Map of Zambia (Fig. 2a), the Map of Agroecological Zones of Somalia (Fig. 2b) and a pair of maps obtained by applying automatic classification algorithms to combinations of amplitude and phase images for both countries. The data in Fig. 7 clearly show that no large differences in vegetation growth can be observed between most agroecological zones.

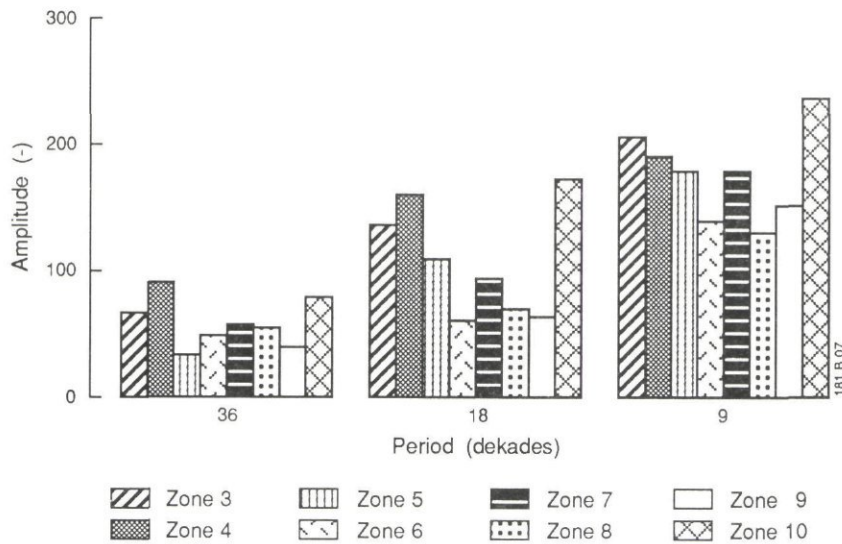


Fig. 7 Fourier spectrum of NDVI time serie; Zambia, 1 Sept. 1983-31 Aug. 1984; dominant components at P=36, 18 and 9 dek. are considered only; a scale factor of 4 respectively of 9 has been applied to values at P=18 respectively 9; agroclimatic zones are the ones of the Agroclimatic Map of Zambia (see Fig. 2a)

Much clearer differences (Fig. 8) can be observed between zones mapped as described in the next section by applying amplitude and phase images in different combinations. Note that although amplitudes at P=36 are rather similar for zones 3 and 4, a large difference is observed at P=18 which gives the possibility of separating zone 3 and 4.

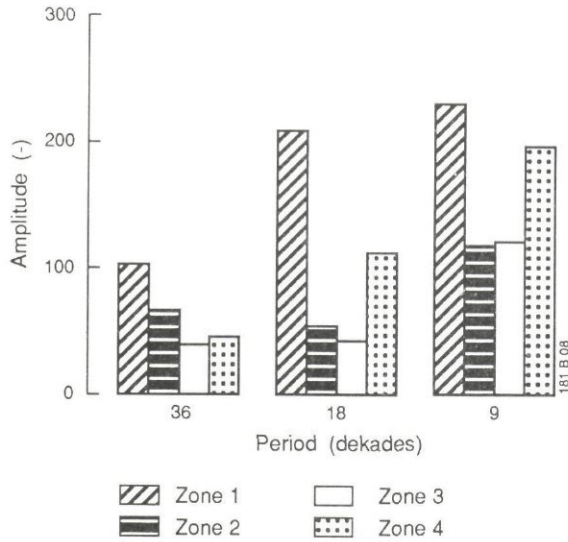


Fig. 8 Fourier spectrum of NDVI time serie; Zambia, 1 Sept.1983-31 Aug. 1984; dominant components at P=36, 18 and 9 dek. are considered only; a scale factor of 4 respectively of 9 has been applied to values at P=18 respectively 9; isogrowth zones mapped as described in Sect. 5

A similar analysis of the mean phase values (Fig. 9) for the agroclimatic zones of Zambia confirms our preliminary conclusions based on amplitude values only. It appears that vegetation development in time was approximately the same (similar amplitude and phase values) in some of the agroclimatic zones, at least in the growing season 1983-1984. This implies that for the purpose of mapping crop growth factors fewer agroclimatic zones should be considered.

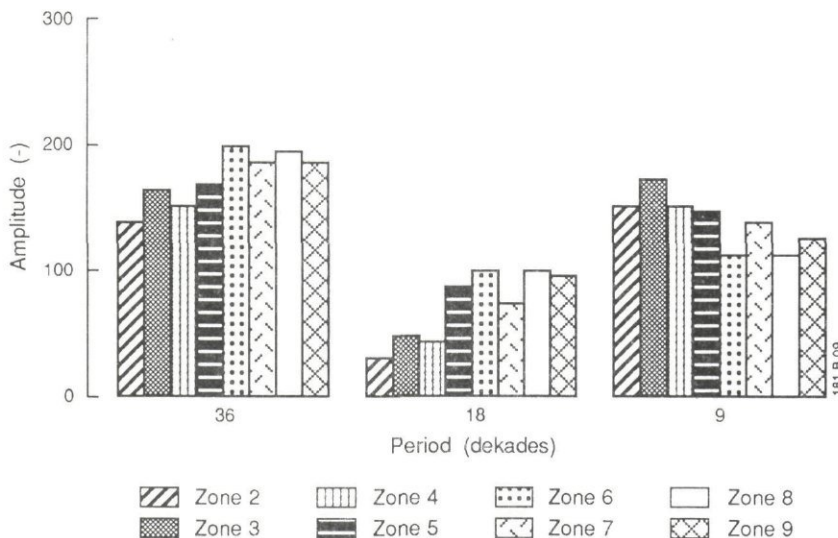


Fig. 9 Mean phase values of agroclimatic zones (see Fig. 2a) of dominant components of vegetation growth at periods P=36, 18 and 9 dekades; Zambia, growing season 1 Sept. 1983 to 31 Aug. 1984

The intricacies of vegetation growth in Somalia, due to higher rainfall variability in time and space are aptly illustrated by means of the mean amplitude values of dominant components (Fig. 10).

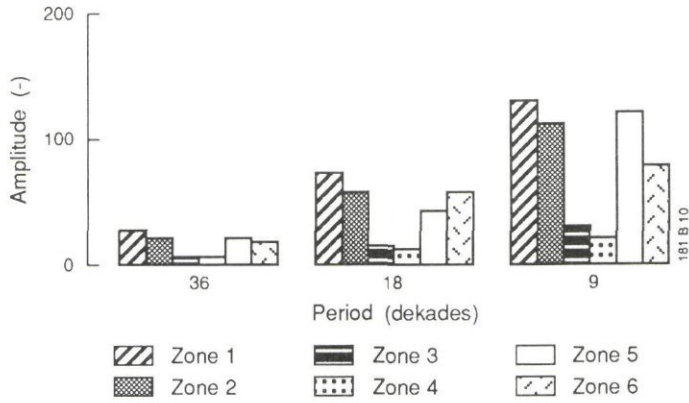


Fig. 10 *Fourier spectrum of NDVI time serie; Somalia, 1 Jan.1984-31 Dec. 1984; dominant components at P=36, 18 and 9 dek. are considered only; a scale factor of 4 respectively of 9 has been applied to values at P=18 respectively 9; the used agroecological zones are some of the map units extracted from the Agroecological Map of Somalia (see Fig. 2b)*

5 MAPPING AGROECOLOGICAL ZONES

Iso-growth zones can be mapped by applying qualitative image interpretation techniques to images as the ones presented in Sect. 3, preferably in combination with other contrast stretching techniques.

Here results obtained by means of classification algorithms will be presented; different pairs of amplitude and phase values at $P=36$, 18 dek. have been chosen as attributes. Training sets have been selected by sampling either the maps in Fig. 2a,b or the images presented in Sect. 3.

A first selection of training sets has been done on the basis of the agroclimatic map of Zambia (Fig. 2a) and taking as attributes amplitude and phase at $P=36$ dek. Image classification has been done by means of a maximum likelihood algorithm and the result is presented in Fig. 11.

It appears that the agroclimatic map is not suitable as a key to select the training sets, as shown by the results obtained for zone "agro 11a": although a large part of this zone is classified correctly, large areas outside "11a" are assigned to the same class. The underlying reason is that agroclimatic zones do not seem to differ much in growth cycle, as described quantitatively by values of amplitude and phase of periodic components of decreasing period ($P=36$, 18 and 9 dek.). This issue will be analyzed in more detail in the next section. Moreover there are major misclassification errors, like the extent of pixels classified as "lake".

A second selection of training sets has been done by sampling the image presented in Fig. 3; pixels were chosen within zones which appeared qualitatively similar, thereby defining a class. As attributes amplitudes at $P=36$, 18 dek. were chosen.

The results are presented in Fig. 12; although the similarity with Fig. 11 is clear, there are a few differences worth to be mentioned. The area classified as "agro 11a" and "agro 11b" appears as class 1 in Fig. 12. The map in Fig. 12 appears much less noisy than Fig. 11, implying that the differences in vegetation growth suggested by the map in Fig. 2a might not be significant.

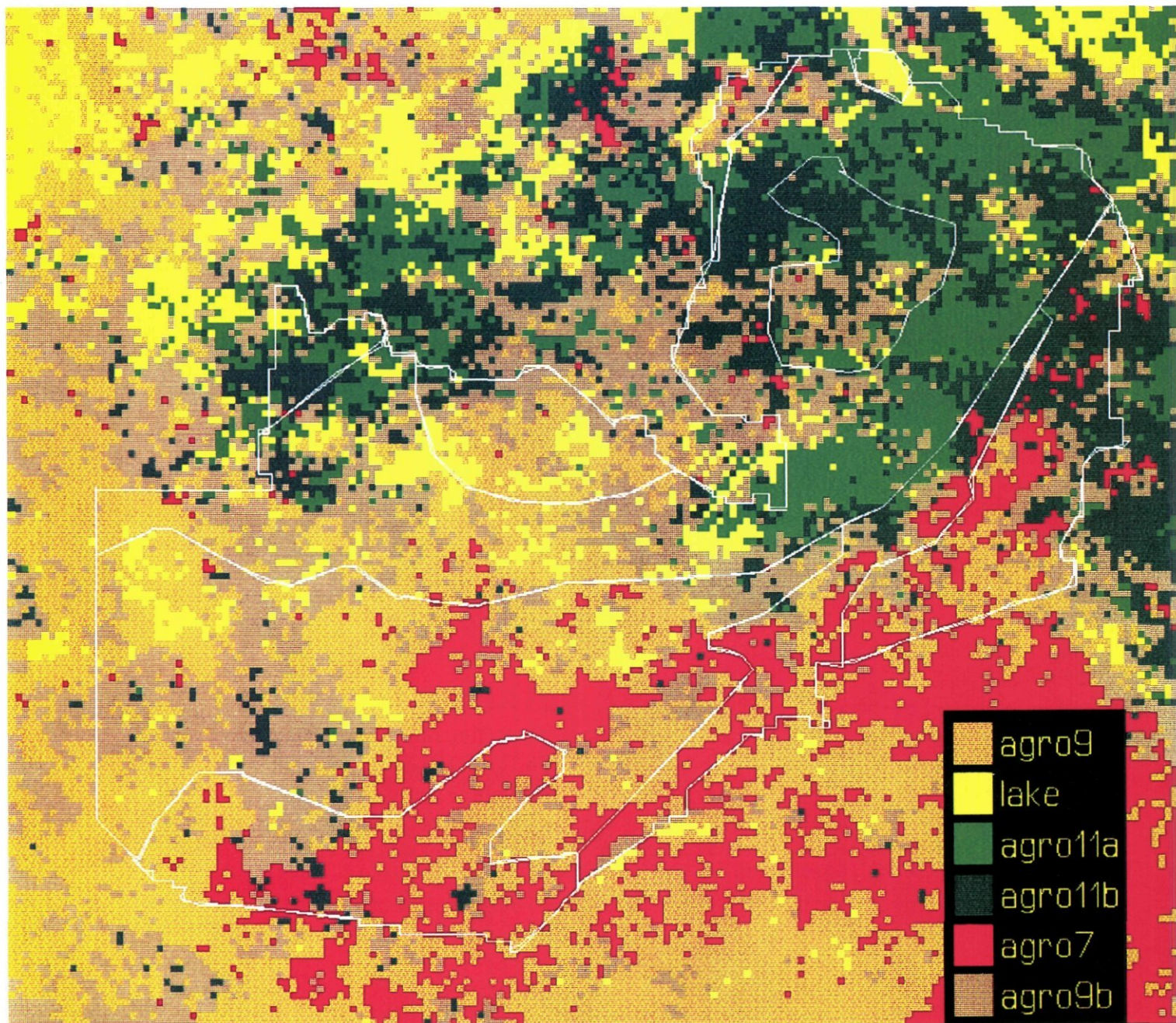


Fig. 11 Map of iso-growth zones obtained by applying a maximum likelihood classification algorithm; attributes: amplitude and phase of yearly component ($P=36$ dek.) of growth cycle, Zambia, Sept. 1983-August 1984; training set: Map of Agroclimatic zones of Zambia (see Fig. 2a)

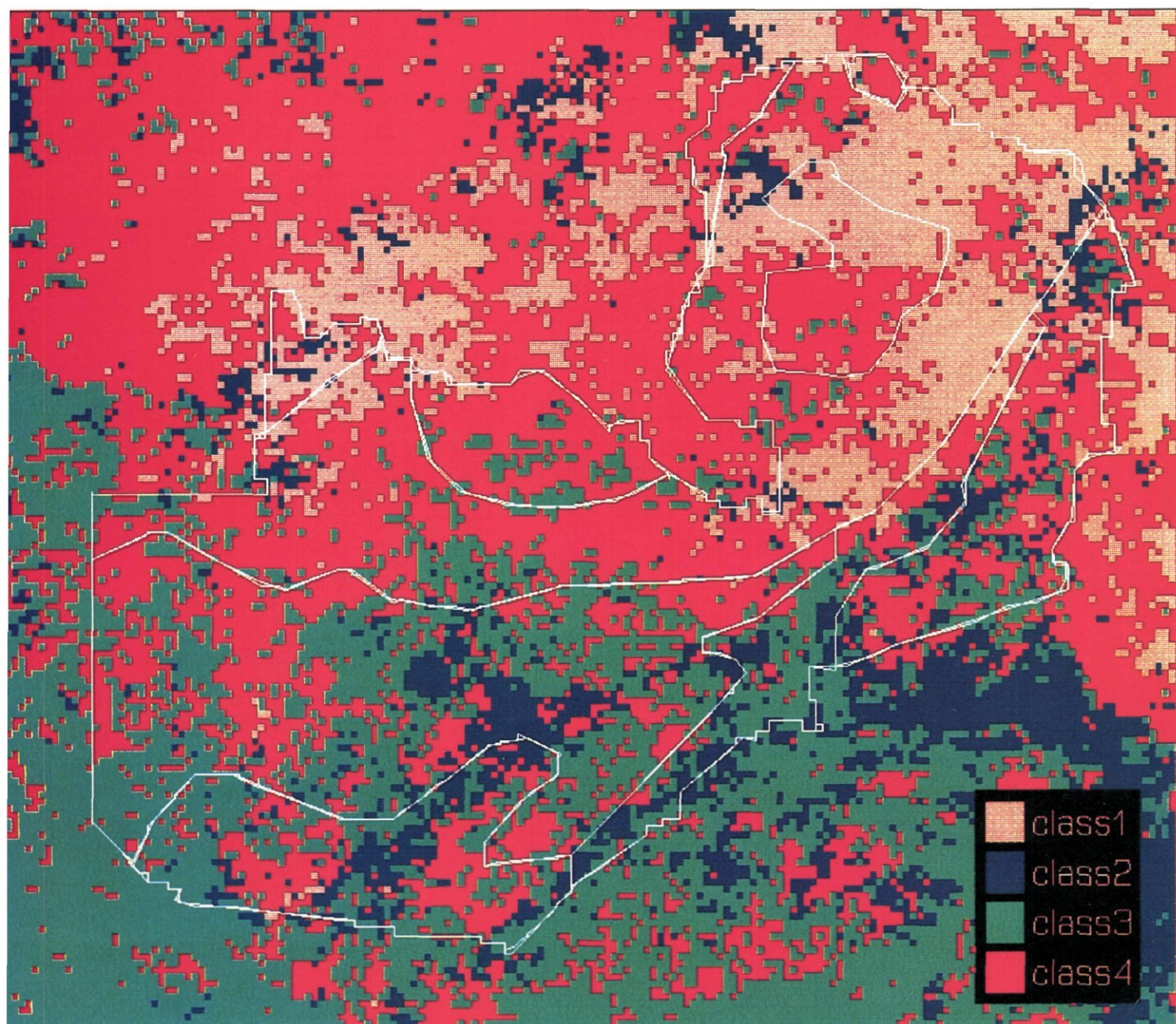


Fig. 12 Map of iso-growth zones obtained by applying a maximum likelihood classification algorithm; attributes: amplitude of yearly ($P=36$ dek.) and six-monthly component ($P=18$ dek.) of growth cycle, Zambia, Sept. 1983-August 1984; training set: colour composite of amplitude and phase at $P=36$ dek. (see also Fig. 3)

6 EVALUATION OF AUTOMATIC CLASSIFICATION METHODS

Amplitude and phase of the harmonics at $P=36$, 18 and 9 dek. can be combined in several ways to map iso-growth zones, as shown in the previous section. Comparison of results in a qualitative fashion, however, is not sufficient to draw a well-founded conclusion on whether map units in Figs. 2a, b do actually relate to differences in vegetation growth. To this purpose, a more detailed assessment has been done on the basis of the mean values and standard deviation of amplitude and phase values of iso-growth zones arising from different combinations of attributes and training sets.

In Fig. 13 mean amplitude values at $P=36$, 18 and 9 dekades of agroclimatic zones as mapped by Schultz (1974) are presented; standard deviations are large in comparison with amplitude values in most cases. This implies that temporal development of green vegetation is rather similar within groups of agroclimatic zones. It appears that significant differences are observed in a very few cases only. This applies, for example, to zones A9 and A10: overlap is relatively small at $P=36$ and 9, while difference is significant at $P=18$.

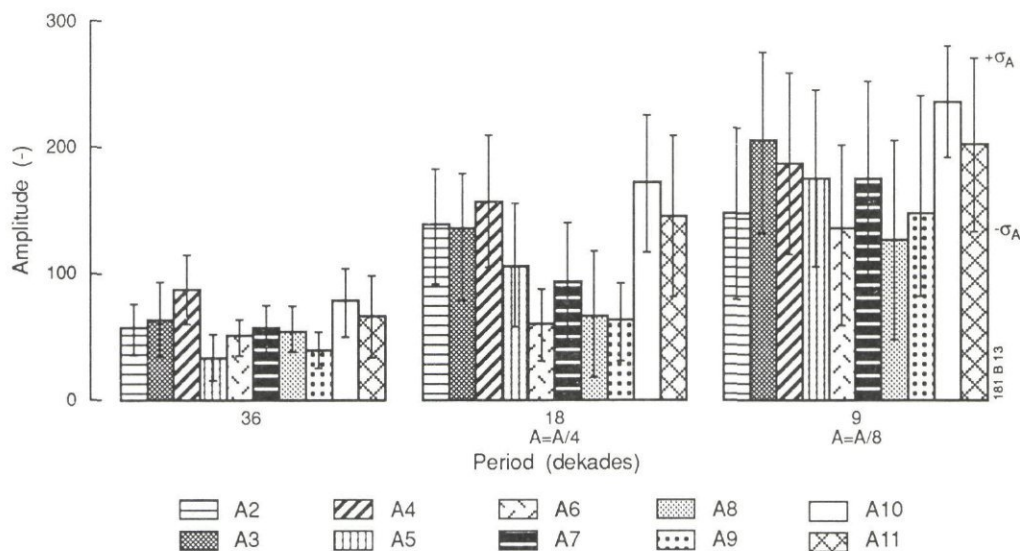


Fig. 13 Fourier spectrum (amplitude) of NDVI time serie; Zambia, 1 Sept. 1983-31 Aug. 1984; dominant components at $P=36$, 18 and 9 dek. are considered only; a scale factor of 4 respectively of 9 has been applied to values at $P=18$ respectively 9; isogrowth zones A_n are the agroclimatic zones mapped by Schultz (1974); vertical bars indicate a range equal to \pm one standard deviation

The same analysis has been repeated by calculating mean amplitude values and standard deviations within the iso-growth zones mapped as described in Sect. 5 (see Fig. 12). The results presented in Fig. 14 indicate that differences in temporal development of green vegetation are much clearer now. It appears that in zones C1 and C4 a strong 6-month component is present, particularly in C1 where the 6-monthly amplitude value is just about half the yearly one. It should be noted that the difference between C3 and

C4 is not significant at P=36 dek., while it clearly is at P=18 dek.; finally C2 and C3 differ significantly at P=36 dek.

It appears that the East-West divide (Fig. 2a) between (I.1) and (I.2, I.3) does correspond to the main North-South difference shown in Fig. 12 in combination with Fig. 13: north of the divide, i.e. in zones C1 and C4, the amplitude of the 6-monthly cycle is larger, while is much smaller than the yearly one south of the divide.

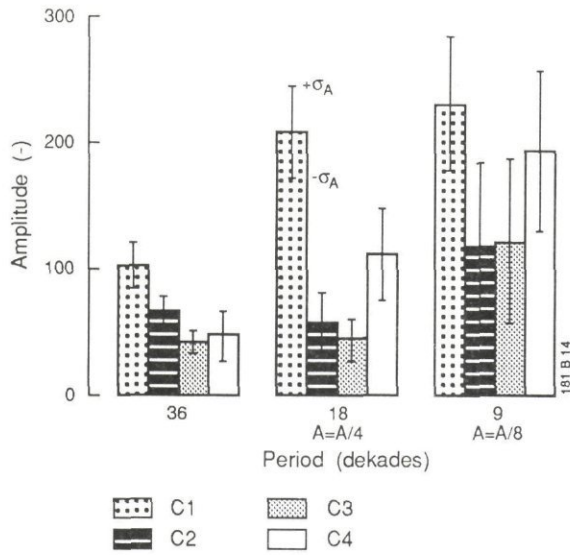


Fig. 14 As Fig. 13; isogrowth zones are the ones of the map presented in Fig. 12

7 CONCLUSIONS

The argument which leads to the conclusions here below can be summarized as follows:

1. The review of literature on analysis of NDVI data (Sect. 1) shows that NDVI is a reliable, direct, measurement of vegetation development.
2. Maps taken as a reference try to combine a number of growth factors, e.g. climate, to identify zones wherein vegetation development should be similar in time and in space. The maps are "indirect" since it is assumed that vegetation reacts consistently to each combination of growth factors.
3. If 2 is true, then different zones should show statistically significant differences in NDVI values or indicators derived herefrom.
4. The maps based on Fourier analysis are obtained through the following procedure:
 - selection of training sets on the basis of e.g. (Fig. 12) colour composite;
 - using as attributes in the automatic classification procedure, independent parameters (in the case of Fig. 12 amplitudes of yearly and six-monthly component).
5. Conclusions are based on the statistical significance of differences in the values of indicators (amplitudes and phase values) derived by means of the Fourier analysis; in the case of both Fig. 13 and 14, these are the amplitudes of periodic components having periods of 36, 18 and 9 dekades; similar results were obtained for other combinations of attributes and test parameters; this was presented because simpler to explain.
6. Differences in amplitude values in Fig. 13 are statistically not significant, because of the overlap of values ± 1 standard deviation; contrarywise differences in Fig. 14 are significant because there is at least one attribute per class for which the overlap at ± 1 standard deviation is zero. Overlap at 2 or 3 standard deviations implies that differences are significant at increasing levels of (statistical) confidence.

The results presented in this report prove that maps of agroecological zones based on indicators which are only indirectly related to vegetation growth are rather inaccurate. The latter means that these maps do not provide a reliable distribution of zones wherein development in time of green vegetation is similar. A much better definition of such zones has been obtained on the basis of the Fourier transform of NDVI time series. The latter conclusion is based on the comparison of mapping results by applying qualitative, e.g. patternwise, and quantitative, e.g. differences in amplitude values against standard deviation, criteria to maps of isogrowth zones obtained by means of several classification procedures. The results obtained for the Zambia case study clearly match major climatic features, e.g. the differences in rainfall regime between North and South, and the time of peak green-up. This is a clear indication of the reliability of the results obtained for the climatologically more complicated case of Somalia. A clear advantage of the method proposed here is that growth-indicators calculated on the basis of the Fourier transform have a very clear mathematical and physical meaning, which makes further analysis easier.

REFERENCES

ANONYMOUS, 1987. *Establishment of an operational satellite remote sensing system to support agricultural production and desert locust monitoring and forecasting*. Rome, Italy, FAO. Progress Report GCP/INT/432/NET Summary of project activities, Nov. 1986-May 1987.

AZZALI, S., 1990a. *High and low resolution satellite images to monitor agricultural land*. Wageningen, (The Netherlands). The Winand Staring Centre. Report 18.

AZZALI, S., 1990b. "Calculation of crop growth indicators in different african climates using remote sensing and meteorological data: case-studies in Zambia and Somalia." *Proc. Int. Symp. Remote Sensing and Water Resources*, Enschede, 20-24 August, (The Netherlands) 375-382.

BERG, A., J.M. GREGOIRE and A. HUBEUX, 1984. *Projet régional Joliba. Programmes CILSS "Prévision des productions rizicoles par télédétection" et "Surveillances des ressources naturelles renouvelable au Sahel"*. Ispra, Italy. Centre Commune de Recherche. Rapport d'activité 31-12-1983/31-12-1984.

BERKHOUT, J.A.A., J. HUYGEN, S. AZZALI and M. MENENTI, 1988. *MARS definition study; results of the preparatory phase*. Wageningen, (The Netherlands). Institute for Land and Water Management Research (ICW). Report 17 (special issue).

BOATWRIGHT, G.O. and V.S. WHITEHEAD, 1986. "Early warning and crop condition assessment research." *IEEE Transactions on Geoscience and Remote Sensing GE 24*, Vol. 1 : 54-64.

BOX, G.E.P. and G.M. JENKINS, 1970. *Time series analysis, forecasting and control*. Holden-Day, San Francisco, Ca, USA.

BRANDT, S. and H.D. DAHMEN, 1989. *Quantum Mechanics on the Personal Computer*. Berlin Heidelberg, (Germany). Springer Verlag.

BROWN R.J. and C. PREVOST, 1985. "Integration of high and low resolution satellite data for crop condition assessment." *Proc. 1985 Machine Processing of Remotely Sensed Data Symp.*: 189-196.

FOURIER, J., 1818. "Note relative aux vibrations des surfaces élastiques et au mouvement des ondes." *Bulletin des Sciences par la Société Philomatique*: 129-136.

GLICK, H.L., J.F. BENCI and R.J. BROWN, 1984. "Operational crop forecasting using remotely sensed imagery." *8th Canadian Symp. on Rem. Sens.*: 331-341.

TOWNSHEND J.R.G. and C.O. JUSTICE, 1986. "Analysis of the dynamics of African vegetation using the Normalized Difference Vegetation Index." *Int. J. of Rem. Sens.*, Vol. 7, 11: 1435-1446.

TUCKER, C.J., J.A. GATLIN and S.R. SCHNEIDER, 1984. "Monitoring vegetation in the Nile delta with NOAA-6 and NOAA-7 AVHRR imagery." *Photogramm. Eng. and Rem. Sens.* Vol. 50, 1: 53-61.

TUCKER, C.J., J.U. HIELKEMA and J. ROFFEY, 1985a. "The potential of satellite remote sensing of ecological conditions for survey and forecasting desert-locust activity." *Int. J. of Rem. Sens.* Vol. 6, 1: 127-138.

TUCKER, C.J., C.L. VANPRAET, M.J. SHARMAN and G.VAN ITTERSUM, 1985b. "Satellite remote sensing of total herbaceous biomass production in the Senegalese Sahel: 1980-1984." *Rem. Sens. of Env.* 17: 233-249.

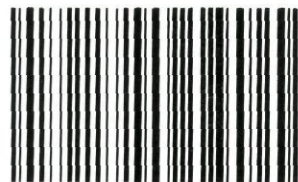
WATSON, R.M., C.I. TIPPETT, J.J. BECKETT, V.SCHOLES, 1979. *The static range resources of the Central rangelands*, London, U.K. Resource management & research. Vol. 1 part 1.

WATSON, R.M. and J.M. NIMMO, 1982. *The static range resources of the Northern rangelands* London, U.K. Resource management & research. Vol. 4 part 1/2.

WATSON, R.M. and J.M. NIMMO, 1985. *The static range resources of the Southern rangelands* London, U.K. Resource management & research. Vol. 1 part 1/1.



Wageningen UR library
P.O.Box 9100
6700 HA Wageningen
the Netherlands
library.wur.nl



10001022563151